Author/s:
Waldeck, K;Cullinane, C;Ardley, K;Shortt, J;Martin, B;Tothill, RW;Li, J;Johnstone, RW;McArthur, GA;Hicks, RJ;Wood, PJ

Title:
Long term, continuous exposure to panobinostat induces terminal differentiation and long term survival in the TH-MYCN neuroblastoma mouse model

Date:
2016-07-01

Citation:
Waldeck, K., Cullinane, C., Ardley, K., Shortt, J., Martin, B., Tothill, R. W., Li, J., Johnstone, R. W., McArthur, G. A., Hicks, R. J. & Wood, P. J. (2016). Long term, continuous exposure to panobinostat induces terminal differentiation and long term survival in the TH-MYCN neuroblastoma mouse model. International Journal of Cancer, 139 (1), pp.194-204. https://doi.org/10.1002/ijc.30056.

Long term, continuous exposure to panobinostat induces terminal differentiation and long term survival in the TH-MYCN neuroblastoma mouse model

K. Waldeck [1], C. Cullinane [1,4], K. Ardley [1], J. Shortt [2,4,5], B. Martin [2], R.W. Tothill [1], J. Li [3], R.W. Johnstone [2,4], G.A. McArthur [1,4,6], R.J. Hicks [1,4], P.J. Wood [1,7,8]

[1] Translational Research, [2] Gene Regulation Laboratories and [3] Bioinformatics Core Facility, Peter MacCallum Cancer Centre, East Melbourne, Victoria, Australia.
[4] Sir Peter MacCallum Department of Oncology, University of Melbourne, Parkville, Victoria, Australia.
[5] School of Clinical Sciences at Monash Health, Monash University, Clayton, Victoria, Australia.
[6] St.Vincent's Hospital, Department of Medicine, Fitzroy, Victoria, Australia.
[7] Children's Cancer Centre, Monash Health, Clayton, Victoria, Australia.
[8] Department of Paediatrics, Monash University, Clayton, Victoria, Australia.

Corresponding author:
Paul J Wood

Paul.Wood@petermac.org
Phone: +61 3 96561517
Fax: +61 3 96561414

Running Title: Panobinostat induces differentiation and long-term survival in neuroblastoma
Keywords: Neuroblastoma, panobinostat, TH-MYCN mouse model, differentiation, HDAC inhibitors
Abbreviations: HDAC – histone deacetylase, HDACi – histone deacetylase inhibitor
Article Category: Research Article - Cancer Therapy and Prevention

The results of our research suggest that epigenetic modulation of murine neuroblastoma via histone deactylase inhibition, promotes a terminal differentiation phenotype in the TH-MYCN mouse model resulting in a sustained survival benefit in over 90% of mice treated. The finding that continuous, prolonged panobinostat exposure is required for this effectiveness raises questions regarding the scheduling currently used for this class of drugs and how such drugs may be best incorporated into current neuroblastoma treatment protocols.

Abstract:

Neuroblastoma is the most common extra-cranial malignancy in childhood and accounts for approximately 15% of childhood cancer deaths. Amplification of MYCN in neuroblastoma is associated with aggressive disease and predicts for poor prognosis. Novel therapeutic approaches are therefore essential to improving patient outcomes in this setting. The histone deacetylases are known to interact with N-Myc and regulate numerous cellular processes via epigenetic modulation, including differentiation. In this study we utilised the TH-MYCN mouse model of neuroblastoma to investigate the antitumour activity of the pan-HDAC inhibitor, panobinostat. In particular we sought to explore the impact of long term, continuous panobinostat exposure on the epigenetically driven differentiation process. Continuous treatment of tumour bearing TH-MYCN transgenic mice with panobinostat for nine weeks led to a significant improvement in survival as compared to mice treated with panobinostat for a three-week period. Panobinostat induced rapid tumour regression with no regrowth observed following a nine-week treatment period. Initial tumour response was associated with apoptosis mediated via up-regulation of BMF and BIM. The process of terminal differentiation of neuroblastoma into benign ganglioneuroma, with a characteristic increase in S100 expression and reduction of N-Myc expression, occurred following prolonged exposure to the drug. RNA-sequencing analysis of tumours from treated animals confirmed significant up-regulation of gene pathways associated with apoptosis and differentiation. Together our data demonstrate the potential of panobinostat as a novel therapeutic strategy for high-risk neuroblastoma patients.

Introduction:

Neuroblastoma is the most common extra-cranial malignancy in childhood and accounts for approximately 15% of childhood cancer deaths [1]. Despite aggressive therapies, including autologous bone marrow transplantation, the outcomes for children who present with advanced disease remains dismal. The amplification of the proto-oncogene MYCN in neuroblastoma remains one of the strongest predictors of poor prognosis [1, 2]. There has been worldwide research focusing on the MYC family of proto-oncogenes and in particular focusing on ways to ameliorate their transcriptional consequences [3, 4]. MYCN transcription can induce a variety of changes in cellular processes including apoptosis and differentiation [5-7]. Therefore modulating MYCN has the potential to reverse the transcriptional processes that are responsible for driving and maintaining malignant neuroblastoma.

Neuroblastoma is a cancer that has the ability to spontaneously differentiate into non-malignant neuronal tissue [1, 2, 8]. This is the characteristic phenotype of stage 4s disease when seen in children less than 18 months old. The hallmark of this stage 4s disease is the absence of MYCN amplification [8]. The potential role of epigenetic regulation in this regression has been considered. Recently presented research focussing on stage 4s disease identified reduced promoter methylation in 97% of the genes in which differential methylation was detected. What is more fascinating is that these samples were enriched for genes known to have binding sites for transcription factors involved in cell differentiation [9]. In addition, whole-genome sequencing of a comprehensive series of neuroblastoma, including both low and high stage tumours, demonstrated that high-grade aggressive tumours had recurrent defects in genes controlling neuritogenesis and therefore, differentiation [10]. The possibility therefore exists for epigenetic modifiers, such as histone deacetylase inhibitors (HDACi), to drive this regression via differentiation. In particular, if this process can be replicated in the more aggressive form of the disease, it might be possible to drive the differentiation process and therefore transform the malignant neuroblastoma into a more benign ganglioneuroma.

The histone deacetylase inhibitors are a class of drugs that target class I, II and IV histone deacetylases (HDACs) in humans. To date numerous proteins have been

identified that are substrates for one or more of the HDACs. These substrates include proteins that have a variety of regulatory roles within the cell that modify important cellular processes. These processes include cell proliferation, migration, differentiation and death [11]. It follows therefore that modification of these HDACs can impact on these cellular processes. The ability of HDACi to induce apoptosis in cancer has been well documented [12]. HDACi have also been shown to synergistically enhance the apoptotic activity of conventional chemotherapeutic agents in neuroblastoma cell lines [13]. There is also evolving evidence to suggest that MYCN and HDACs co-operate to regulate these cellular processes, including cellular differentiation. In particular HDAC5, a class II HDAC, has been shown to block neuroblastoma cell differentiation by co-operating with MYCN [14]. Further to this, selective inhibition of HDACs, including HDAC8, have been shown to induce neuroblastoma differentiation [15, 16]. This is consistent with the observation that neuroblastoma cells with over-expressed MYCN retain their capacity to undergo differentiation [17]. This ability to drive the differentiation process has been observed in other cancer types including acute myeloid leukemia (AML) and osteosarcoma [18, 19]. In particular, terminal differentiation of osteosarcoma cells is seen following sustained, low dose treatment with HDACi [19].

In this study we utilised the TH-MYCN mouse model of neuroblastoma which has been shown to closely replicate the clinical form of the disease both in its behaviour as well as genetic characteristics [20] to investigate the antitumour activity of the pan-HDACi, panobinostat, and further, to investigate the role of terminal differentiation in this response. In particular we sought to explore the impact of long term, continuous panobinostat exposure on the epigenetically driven differentiation process.

Methods:

TH-MYCN mouse model and cell lines

The TH-MYCN neuroblastoma mouse model (on an SV129 background) [20, 21] and NH02A cells [22] were kindly provided by Professor Michelle Haber (Children's Cancer Institute, Australia). The IMR32 human neuroblastoma cell line was purchased from DSMZ (Germany). All animal experiments were carried out with institutional animal ethics committee approval. Mice were genotyped at 4 weeks of age and homozygous mice monitored by ultrasound imaging for tumour development. Ultrasound images were obtained using the Visualsonics® VEVO 770-230 high-resolution imaging system, which in turn calculates 3D volumetric measurements. A tumour volume of less than 50mm^3 on ultrasound imaging was assigned as 'below the limit of detection'. Once tumours reached a volume of between 50-200 mm^3 the mice were randomised to receive vehicle or 5 mg/kg panobinostat (Selleck Chemicals) by intraperitoneal injection daily for either 3 or 9 weeks. Tumour growth was monitored by ultrasound imaging twice weekly during therapy and once weekly thereafter. The mice were euthanized when tumour volumes exceeded 600mm^3, or on day 163 (end point). For short term studies, animals were euthanized at 4 hr post the final drug dose for collection of tumour samples.

Cell death analysis

Cells treated with panobinostat (Selleck Chemicals), with or without the addition of the pan-caspase inhibitor Q-VD-OPh (Merck Millipore), for 48 hr were fixed in 70% ethanol then stained with propidium iodide (in PBS containing RNAse) before being analysed using a Canto II FACS analyser. Analysis was performed using FCS Express software (version 3). Sub-G1 population was determined as an indicator of cell death.

Western Blot Analysis

Cells were treated with either panobinostat or vorinostat (Selleck Chemicals) lysed into either RIPA or RAC buffer, separated by SDS-PAGE and western blotting performed with anti-actin (1:10000, MP Biomedicals #69100), caspase 3 (1:1000, Cell Signaling #9662), Bcl-2 (1:1000, Cell Signaling #2870), BIM (1:1000, Cell Signaling #2933), Mcl-1 (1:1000, Cell Signaling #5453), BMF (1:500, Enzo Life Sciences ALX-804-508) and Acetyl Histone H3 (1:2000, Merck Millipore #06-599)

antibodies. Immunoreactive proteins were visualized on x-ray film using ECL reagents (Amersham).

Quantitative Real-Time PCR

RNA from cells and tumours was prepared using the High Pure RNA Isolation kit (Roche) and High Pure Tissue Isolation kit (Roche), respectively. cDNA synthesis and quantitative real-time PCR reactions, performed using the SYBR Green (Applied Biosystems) detection method in a StepOne PCR machine (Applied Biosystems) were as previously described [23]. Average Ct values for each of the three replicates per sample were calculated, relative to the expression of the ribosomal protein L32. Fold change expression was determined using the 2^deltaCT method, with expression changes relative to control untreated cells/tumours. Results are shown as mean +/- SEM of at least three individual experiments/tumours.

Immunohistochemical analysis

FFPE tumour sections (4 μm) were stained using antibodies to cleaved caspase 3 (1:250, Cell Signaling #9664), N-Myc (1:200, Calbiochem OP13), S100 (1:3000, Dako Z0311), SSTR2 (1:250, Abcam #134152), Enolase 2 (NSE; 1:500, Thermo Scientific PA5-27452), and Ki67 (1:2000, Novacastra NCL-Ki67p). The slides were then incubated with the appropriate secondary antibody, followed by DAB Chromogen reagent (Dako). Tumour sections were also stained with Heamatoxylin and Eosin (H&E). Images were captured on a BX-61 Olympus microscope at 40x magnification.

TUNEL assay

FFPE tumour sections (4 μm), and cytospins of panobinostat treated NH02A and IMR32 neuroblastoma cells, and vorinostat treated NH02A cells, were stained with the ApopTaq Peroxidase In Situ Apoptosis Detection kit (TUNEL assay; Millipore #S7100) as per manufacturers instructions. Images were captured on a BX-61 Olympus microscope at 40x magnification. Percent of cells stained positively was calculated using Meta Imaging Series 6.1 software.

RNA sequencing and data analysis

RNA was extracted from four baseline and four panobinostat treated tumours (24hr timepoint). Tumour bearing mice were treated with two doses of either vehicle or 5 mg/kg panobinostat 24 hr apart. At 4 hr following the second dose the animals were euthanized and tumours taken and snap frozen for RNA analysis. RNA was extracted using the Qiagen miRNAeasy kit and quality assessed using the Agilent 2100 Bioanalyzer (Agilent Technologies). RNA sequencing (RNA-seq) libraries were prepared using the IlluminaTruSeq V2 RNA-Seq sample preparation kit, and paired-end 50bp RNA-seq reads were generated using HiSeq 2500 (mean read coverage 51719340). Reads were quality checked by FastQC and trimmed if necessary for low base quality or adaptor using Cutadapt v1.6 [24]. Alignment was then performed against the mouse reference genome GRCm38 using TopHat (v2.0.12) [25] with maxmultihits set to 1 and using the option to map first to the reference transcriptome. HTSeq v0.5.4p5 [26] with mode intersection-nonempty used to count the number of reads per gene using gene definition from Ensembl Release 73. Prior to differential expression analysis genes with very low counts were removed; genes with more than 1 cpm in at least 2 samples were used for analysis. The limma-voom method v3.22.1 [27] was used to identify differentially expressed genes. Gene Set Enrichment Analysis (GSEA) [28, 29], was performed over the MSigDB C2 gene sets with the additional HDAC inhibitor differentiation gene signature published by Frumm *et al* [15]. Pathway mapping of significant genes (p value <0.05, expression fold change threshold 0.25) was undertaken using GeneGo Metacore software. RNA-seq data is made publicly available (GEO accession number GSE69869).

Statistical analysis

Statistical significance was determined by one-way ANOVA with Dunnett's post hoc analysis versus control, or by Student *t*-test. Analysis was performed using GraphPad Prism Version 6.01 software.

Results:

Treatment with panobinostat results in caspase 3 dependent apoptosis in neuroblastoma cells.

The NH02A cell line which is derived from the TH-MYCN murine neuroblastoma model, and the IMR32 human neuroblastoma cell line, were investigated for their sensitivity to the pan-HDACi, panobinostat. Both cell lines were highly sensitive to panobinostat, demonstrating IC_{50}'s of 6.9 ± 4.5 nM and 8.9 ± 4.2 nM, respectively (Fig S1a), a sensitivity range similar to that previously demonstrated for human neuroblastoma lines [13]. Panobinostat treatment resulted in dose dependent cell death as evidenced by the increasing proportion of cells with sub-G1 DNA content in both cell lines (Fig 1a and b, Fig S2a and b). Indeed, treatment of NH02A and IMR32 cells with 50 nM panobinostat induced 38.5% and 39.5% cell death, respectively. This cell death was confirmed as being caspase dependent, with the proportion of cells with sub-G1 DNA content reduced back to control levels after treatment with panobinostat in combination with the caspase inhibitor q-VD-OPh (Fig 1a and b, Fig S2a and b). Furthermore, at doses of panobinostat that increased acetylation of histone H3 at 4 hr (10 and 50 nM), the resulting cell death, in both the NH02A and IMR32 cells, at 48 hr was associated with an increase in cleaved caspase 3, (Fig 1c, Fig S2c). Positive TUNEL staining after 24 hr of 50 nM panobinostat treatment further confirmed the induction of apoptosis, with 12.5% of NH02A and 14% of IMR32 cells staining positively (Fig 1d, Fig S2d). Similar studies in the NH02A cell line with the HDAC inhibitor vorinostat showed an induction of apoptosis in response to treatment, with increased cleaved caspase 3 and TUNEL assay positivity observed (Fig S1a, b and c), confirming that effects observed are mediated by HDAC inhibition.

HDAC inhibitors have been shown to regulate apoptosis through up-regulation of the pro-apoptotic proteins BIM and BMF and down regulation of the anti-apoptotic proteins Bcl-2 and Mcl-1, depending on the cell line and drug used (Reviewed in Matthews *et al*, [30]). Most significantly, panobinostat has been shown to upregulate BMF [23, 31]. To determine whether these same mechanisms for the regulation of apoptosis occur in neuroblastoma cells, NH02A and IMR32 cells were treated for up to 24 hr with 5 nM of panobinostat and analysed for expression of apoptotic proteins. Expression of BIM (EL, L and S forms) was increased in response to panobinostat,

with the highest expression level observed after 24 hr of treatment (Fig 1e and Fig S2e). Interestingly Mcl-1 expression was also seen to increase over time, though this increase was more pronounced in the NH02A cells as compared to the IMR32 cells, while Bcl-2 levels remained unchanged (Fig 1e and Fig S2e). mRNA expression has been used extensively to determine BMF expression in response to HDAC inhibitors [23, 31]. In NH02A cells, BMF mRNA expression increased 10.4-fold above control levels after 4 hr of treatment with 5 nM panobinostat (P <0.001), with this level only slightly decreasing out to 24 hr (Fig 1f). While BMF mRNA increased 7.8-fold above control levels after 4 hr of 5 nM panobinostat treatment in the IMR32 cells (P <0.001; Fig S2f).

Panobinostat treatment of TH-MYCN tumour bearing mice prolongs disease free survival.

Transgenic mice homozygous for N-Myc expression in the developing neural crest (TH-MYCN) develop neuroblastomas by 6 weeks of age and typically succumb to their disease very rapidly [20]. To determine the efficacy of panobinostat in the TH-MYCN neuroblastoma model, homozygous mice with demonstrable disease were randomized to receive vehicle or 5 mg/kg of panobinostat daily, a dose previously determined as a well tolerated dose for this model (Fig S3a) for a total of three or nine weeks. Mice were randomized based on tumour volume as determined by ultrasound imaging with the average tumour volume not significantly different between the groups at baseline (P >0.05, Fig 2a). Tumours in the vehicle treated group grew rapidly with a median time to sacrifice due to tumour burden of 7 days (Fig 2b). In contrast, panobinostat treatment was associated with rapid tumour regression on ultrasound imaging with no tumour detectable by day 5 of therapy (Fig 2b). Mice treated with panobinostat for 3 weeks remained tumour free throughout the therapy window, however the animals began to relapse with neuroblastoma after this period (Fig 2c). This treatment regimen however resulted in a significant increase in median survival to 68 days (P <0.0001 vs vehicle).

To investigate whether a longer period of panobinostat therapy would lead to further improvement in antitumour efficacy, tumour bearing TH-MYCN mice were treated continuously for 9 weeks. Panobinostat was well tolerated on this regimen, with minimal weight loss observed during treatment (Fig S3b). As observed with the 3

week schedule, no tumour regrowth occurred during the treatment period. However, with the exception of one mouse, which relapsed within 6 days of the completion of treatment, no tumour regrowth was observed at 100 days post cessation of treatment (Fig 2c). This treatment schedule resulted in a significant improvement in survival compared with the 3 week dosing schedule (P <0.0001) and potentially, a curative response. Analysis of the single relapsed tumour revealed no acetylation of histone H3, and the characteristic histology and N-Myc expression of TH-MYCN neuroblastoma (Fig S3c and d).

*Panobinostat treatment in the TH-MYCN mouse model results in a rapid apoptotic response***.**

On the basis of the *in vitro* findings and the rapid tumour regression observed upon panobinostat treatment *in vivo*, tumours were analysed for markers of apoptosis. Immunostaining of tumour sections showed a dramatic increase in expression of cleaved caspase 3, as well as TUNEL assay positivity (Fig 3a), at 24 hr post treatment and this correlated with histologic changes typical of apoptosis (such as nuclear fragmentation) as seen in the H&E sections (Fig 3a). To investigate whether the apoptosis observed was mediated through mechanisms similar to those seen *in vitro*, tumour expression of the pro- and anti-apoptotic proteins BMF, BIM, Bcl-2 and Mcl-1 was determined. As seen in Fig 3b, and consistent with the *in vitro* findings, panobinostat robustly induced histone H3 expression while BIM, Mcl-1 and BMF protein levels were increased and Bcl-2 remained unaltered. Additionally, BMF mRNA expression was increased 3 fold as compared to baseline (P <0.05, Fig 3c).

Long term treatment of the TH-MYCN mouse model with panobinostat results in differentiation.

While the initial response to panobinostat is consistent with an apoptotic phenotype, the differences in survival and relapse between the mice treated with 3 and 9 weeks of therapy suggests that a second process may be required for relapse free survival. There is emerging evidence that HDACi therapy causes differentiation of neuroblastoma cells [14-16]. To assess whether differentiation occurs in response to panobinostat, tumours were analysed for markers of differentiation. Samples collected from the tumour site on day 21 and at the endpoint of the 9 week therapy study (day 163, endpoint) comprised small white nodules which upon histological analysis were

confirmed to harbour large areas of calcification (data not shown). H&E staining (Fig 4) revealed that the poorly differentiated neuroblastoma histology observed in vehicle treated tumours was altered upon panobinostat therapy, to include ganglion cells surrounded by schwannian stroma, suggestive of a well-differentiated phenotype consistent with ganglioneuroma. Indeed, at day 7 of treatment, samples from the tumour site show evidence of both poorly and well differentiated cell types, with pockets of differentiated ganglion cells present adjacent to nodes of neuroblastoma cells (Fig S4a). Immunostaining revealed the number of N-Myc expressing, Ki67 positive neuroblastoma cells was reduced by day 7, with no pockets of neuroblastoma cells evident at day 21 or endpoint (Fig 4, Fig S4b). In contrast, the expression of the differentiation markers, S100, somatostatin receptor 2 (SSTR2), and Enolase 2 (NSE) was evident by day 7 and increased further at the later time points (Fig 4). As expression of the differentiation markers was associated with the ganglion cells and schwannian stroma, these data strongly support the induction of differentiation during panobinostat treatment.

To further investigate neuroblastoma cell differentiation in response to panobinostat, RNA-seq analysis was performed. Differential gene expression analysis was performed on tumours harvested at baseline and following two doses of panobinostat given 24 hr apart. This data confirmed the earlier findings of increased expression of BIM, BMF and S100, and decreased expression of N-Myc and Ki67 upon drug treatment (Supplementary table 1; RT-PCR validation of MYCN and downstream targets of MYCN expression, Pol1rb and ODC [32-34], Fig S5a, b and c). Pathway enrichment analysis revealed that genes involved in cell cycle regulation, neurogenesis and axonal guidance, chromatin modification, cytoskeletal remodelling and the NOTCH signalling pathway were significantly altered after panobinostat treatment (Fig 5a, Fig S5d). Furthermore, specific GSEA analysis comparing the data from this study with the HDACi differentiation gene signature developed by Frumm *et al* [15], showed that the up-regulated genes of that signature are significantly enriched for within the current data set (Normalised Enrichment Score 1.56, P= 0.019, FDR q-value 0.042, Fig 5b). While the Frumm differentiation gene signature includes 59 genes, our analysis reduced this to 41 genes, upon exclusion of 8 control genes and a further 10 genes without a mouse homologue or due to gene expression below the limit of detection. Direct comparisons between these two data sets showed that 66%

of the genes were altered in expression in the same direction (27/41 genes, Fig 5c), with 68% of the up-regulated genes identified by Frumm *et al* also up-regulated in the TH-MYCN model in response to panobinostat (21/31) and 60% of down-regulated genes being present in both (6/10, Fig 5c, bottom panel). Together these data strongly suggest the initial induction of differentiation in TH-MYCN tumours by panobinostat starts as early as 24 hr.

Discussion:

Despite recent advances in the treatment of neuroblastoma, patients who present with advanced disease continue to have a poor prognosis. In particular, patients with a poor, or no, response after standard induction chemotherapy, have an overall survival of less than 10 percent [35, 36]. Due to the infiltrating behaviour of the primary tumour, which often encroaches on multiple essential structures, a complete surgical resection is often impossible, inevitably leaving residual tumour deposits behind. Thus there is an evolving need to find alternate therapies in this subset of children in whom residual disease imparts a dismal prognosis.

Neuroblastoma, ganglioneuroblastoma and ganglioneuroma constitute an inclusive spectrum of diseases that differ in their degree of maturation [37]. Ganglioneuroma, the most mature and therefore differentiated entity of this spectrum is considered a benign tumour [37]. The ability of undifferentiated neuroblastoma, in infants less than 18 months old with stage 4s disease, to spontaneously differentiate into a more differentiated entity is well documented [8]. If this process can be emulated in older children with residual disease, it may be possible to drive the residual malignant neuroblastoma into a more benign lesion thus reducing its potential to cause harm.

Inducing differentiation in neuroblastoma is not a new concept. Retinoids have been included as a post-consolidation, metronomic therapy in high-risk neuroblastoma protocols for this very reason [38]. To date retinoids have the strongest evidence to be considered for this role. However they have inherent toxicities that are often difficult for young children to tolerate. Newer agents such as fenretinide may reduce this toxicity [38]. Targeted therapies are now emerging as a potential alternative to retinoic acids, and these agents include HDAC inhibitors such as panobinostat. Indeed

epigenetic modification of neuroblastoma may be the key to driving a terminal differentiation process as early results from the study of the characteristic methylomes of stage 4s patients suggest [9]. HDACi have been extensively evaluated in neuroblastoma using both pre-clinical models and early phase studies, however the bulk of this testing has been performed using an intermittent dosing schedule [39]. Recent pre-clinical evidence suggests that these agents are more effective as differentiating agents in continuous low doses, rather than higher intermittent dosing [19]. Such a dosing schedule could also translate to a lower spectrum of side effects, potentially making HDAC inhibitors less toxic.

Our results suggest that continuous, low dosing of single agent panobinostat induces terminal differentiation in a murine model of neuroblastoma. To date, this appears to be a unique result for single agent therapy in this aggressive mouse model of neuroblastoma. In addition, the process of terminal differentiation appears to be time and therefore exposure dependent. Mice treated continuously for three weeks had an impressive initial response but eventually all relapsed with aggressive disease. If this therapy was extended to nine weeks, 90% of mice remained in remission. When these mice were examined, they had tumour remnants, too small to be accurately identified by ultrasound, that were histologically consistent with a benign, well-differentiated ganglioneuroma.

The time dependent nature of this response is in itself interesting. RNA-seq analysis performed as early as 24 hours after panobinostat dosing in vivo, suggests that some pathways involved in differentiation are already significantly up-regulated. However, despite these early changes to differentiation pathways, the terminal differentiation observed in the TH-MYCN neuroblastoma tumours requires prolonged exposure to HDACi to become permanent. More specifically, pathways such as NOTCH signalling, well documented as being a promoter of differentiation [40], appear significantly up-regulated. This up-regulation of NOTCH signalling is confirmed on mRNA analysis of treated tissue. It is important to note that pathways associated with cell cycle arrest and apoptosis are also significantly altered suggesting a dual role for HDAC inhibition. The initial, dramatic tumour response can potentially be explained by a predominantly apoptosis phenotype. The ongoing, sustained effect in those mice that eventually remain disease-free can be explained by a predominantly

differentiation phenotype. The apoptosis effect on its own does not appear sufficient to sustain a prolonged response as evidenced by the 100% relapse rate in treated mice if therapy is ceased after three weeks. Therefore the length of exposure rather than the degree of exposure determines the balance between the apoptosis and differentiation phenotypes, and therefore the ultimate success of the treatment.

The importance of these findings lies in the concept that current HDACi therapies, by the nature of their intermittent dosing schedule, are not adequately delivering the continuous exposure required for the epigenetically driven process of terminal differentiation to take place in an irreversible manner.

MYCN amplification status has repeatedly been shown to impart a significant prognostic impact on patients with neuroblastoma [41]. Consequently significant research effort has been invested into finding ways to ameliorate the impact of MYCN status in high-risk patients. Interestingly, our results suggest that panobinostat, in addition to its impact on differentiation pathways, has the ability to reduce the translational impact of MYCN as evidenced by a significant reduction in N-Myc expression. Recent research has also demonstrated that this impact of panobinostat on N-Myc expression can be synergistically enhanced when combined with the BET bromodomain inhibitor JQ1 [42]. HDACi have also been shown to influence the expression levels of c-Myc [43] such that this translational effect of panobinostat could potentially be extended to other pediatric cancers such as Medulloblastoma and diffuse intrinsic pontine glioma (DIPG). Additionally, the upregulation of SSTR2 in response to panobinostat might provide for an additional diagnostic and therapeutic target, with somatostatin receptor imaging and peptide receptor radionuclide therapy being previously identified as options in neuroblastoma [44].

Panobinostat has now been extensively studied in both adults and children and has been shown to be a safe and efficacious [45], having been recently FDA approved for use in multiple myeloma [46, 47]. An oral formulation of the drug is now available which is even more suitable for sustained dosing. In addition, oral formulations of drugs are less traumatic to deliver to the pediatric population than intra-venous formulations. When deciding what phase of treatment is most appropriate for incorporation of HDACi therapy it is important to consider their side-effect profile. Currently one of

the most frequent dose limiting side-effects of panobinostat includes bone marrow suppression, in particular neutropaenia and thrombocytopaenia. The initial induction phase of most high-risk protocols is intense and in itself results in significant bone marrow suppression. Therefore, if the aim is to expose patients to continuous HDAC inhibition this may be impossible to achieve until after the end of consolidation therapy. Currently metronomic treatments are scheduled in the post consolidation phase and currently run along side immunotherapy [48]. This is a phase of treatment that is traditionally not complicated by bone marrow suppression and is therefore ideal for the addition of a metronomic therapy. From a translational stand point this provides an excellent opportunity to explore the incorporation of panobinostat into current post-consolidation therapies as an alternative to retinoic acids in the clinical setting.

Acknowledgements:

The authors wish to thank Laura Kirby and the staff of the Peter MacCallum Cancer Centre Flow Cytometry Core Facility for their technical assistance.

References:

1. Maris JM, Hogarty MD, Bagatell R, Cohn SL. Neuroblastoma. *Lancet* 2007;**369**: 2106-20.

2. Brodeur GM. Neuroblastoma: biological insights into a clinical enigma. *Nature reviews Cancer* 2003;**3**: 203-16.

3. Eilers M, Eisenman RN. Myc's broad reach. *Genes & development* 2008;**22**: 2755-66.

4. Vita M, Henriksson M. The Myc oncoprotein as a therapeutic target for human cancer. *Seminars in cancer biology* 2006;**16**: 318-30.

5. Adhikary S, Eilers M. Transcriptional regulation and transformation by Myc proteins. *Nature reviews Molecular cell biology* 2005;**6**: 635-45.

6. Arvanitis C, Felsher DW. Conditional transgenic models define how MYC initiates and maintains tumorigenesis. *Seminars in cancer biology* 2006;**16**: 313-7.

7. Cowling VH, Cole MD. Mechanism of transcriptional activation by the Myc oncoproteins. *Seminars in cancer biology* 2006;**16**: 242-52.

8. Schleiermacher G, Rubie H, Hartmann O, Bergeron C, Chastagner P, Mechinaud F, Michon J. Treatment of stage 4s neuroblastoma--report of 10 years' experience of the French Society of Paediatric Oncology (SFOP). *British journal of cancer* 2003;**89**: 470-6.

9. Brodeur GM, Bagatell R. Mechanisms of neuroblastoma regression. *Nature reviews Clinical oncology* 2014;**11**: 704-13.

10. Molenaar JJ, Koster J, Zwijnenburg DA, van Sluis P, Valentijn LJ, van der Ploeg I, Hamdi M, van Nes J, Westerman BA, van Arkel J, Ebus ME, Haneveld F, et al. Sequencing of neuroblastoma identifies chromothripsis and defects in neuritogenesis genes. *Nature* 2012;**483**: 589-93.

11. Dokmanovic M, Clarke C, Marks PA. Histone deacetylase inhibitors: overview and perspectives. *Molecular cancer research : MCR* 2007;**5**: 981-9.

12. Bolden JE, Peart MJ, Johnstone RW. Anticancer activities of histone deacetylase inhibitors. *Nature reviews Drug discovery* 2006;**5**: 769-84.

13. Wang G, Edwards H, Caldwell JT, Buck SA, Qing WY, Taub JW, Ge Y, Wang Z. Panobinostat synergistically enhances the cytotoxic effects of cisplatin, doxorubicin or etoposide on high-risk neuroblastoma cells. *PloS one* 2013;**8**: e76662.

14. Sun Y, Liu PY, Scarlett CJ, Malyukova A, Liu B, Marshall GM, MacKenzie KL, Biankin AV, Liu T. Histone deacetylase 5 blocks neuroblastoma cell differentiation by interacting with N-Myc. *Oncogene* 2014;**33**: 2987-94.

15. Frumm SM, Fan ZP, Ross KN, Duvall JR, Gupta S, VerPlank L, Suh BC, Holson E, Wagner FF, Smith WB, Paranal RM, Bassil CF, et al. Selective HDAC1/HDAC2 inhibitors induce neuroblastoma differentiation. *Chemistry & biology* 2013;**20**: 713-25.

16. Rettig I, Koeneke E, Trippel F, Mueller WC, Burhenne J, Kopp-Schneider A, Fabian J, Schober A, Fernekorn U, von Deimling A, Deubzer HE, Milde T, et al. Selective inhibition of HDAC8 decreases neuroblastoma growth in vitro and in vivo and enhances retinoic acid-mediated differentiation. *Cell death & disease* 2015;**6**: e1657.

17. Edsjo A, Holmquist L, Pahlman S. Neuroblastoma as an experimental model for neuronal differentiation and hypoxia-induced tumor cell dedifferentiation. *Seminars in cancer biology* 2007;**17**: 248-56.

18. Bots M, Verbrugge I, Martin BP, Salmon JM, Ghisi M, Baker A, Stanley K, Shortt J, Ossenkoppele GJ, Zuber J, Rappaport AR, Atadja P, et al. Differentiation therapy for the treatment of t(8;21) acute myeloid leukemia using histone deacetylase inhibitors. *Blood* 2014;**123**: 1341-52.

19. Cain JE, McCaw A, Jayasekara WS, Rossello FJ, Marini KD, Irving AT, Kansara M, Thomas DM, Ashley DM, Watkins DN. Sustained Low-Dose Treatment with the Histone Deacetylase Inhibitor LBH589 Induces Terminal Differentiation of Osteosarcoma Cells. *Sarcoma* 2013;**2013**: 608964.

20. Rasmuson A, Segerstrom L, Nethander M, Finnman J, Elfman LH, Javanmardi N, Nilsson S, Johnsen JI, Martinsson T, Kogner P. Tumor development, growth characteristics and spectrum of genetic aberrations in the TH-MYCN mouse model of neuroblastoma. *PloS one* 2012;**7**: e51297.

21. Weiss WA, Aldape K, Mohapatra G, Feuerstein BG, Bishop JM. Targeted expression of MYCN causes neuroblastoma in transgenic mice. *The EMBO journal* 1997;**16**: 2985-95.

22. Cheng AJ, Cheng NC, Ford J, Smith J, Murray JE, Flemming C, Lastowska M, Jackson MS, Hackett CS, Weiss WA, Marshall GM, Kees UR, et al. Cell lines from MYCN transgenic murine tumours reflect the molecular and biological characteristics of human neuroblastoma. *Eur J Cancer* 2007;**43**: 1467-75.

23. Bolden JE, Shi W, Jankowski K, Kan CY, Cluse L, Martin BP, MacKenzie KL, Smyth GK, Johnstone RW. HDAC inhibitors induce tumor-cell-selective pro-apoptotic transcriptional responses. *Cell death & disease* 2013;**4**: e519.

24. Martin M. Cutadapt removes adapter sequences from high-throughput sequencing reads. *2011* 2011;**17**.

25. Kim D, Pertea G, Trapnell C, Pimentel H, Kelley R, Salzberg SL. TopHat2: accurate alignment of transcriptomes in the presence of insertions, deletions and gene fusions. *Genome biology* 2013;**14**: R36.

26. Anders S, Pyl PT, Huber W. HTSeq-a Python framework to work with high-throughput sequencing data. *Bioinformatics* 2015;**31**: 166-9.

27. Law CW, Chen Y, Shi W, Smyth GK. voom: Precision weights unlock linear model analysis tools for RNA-seq read counts. *Genome biology* 2014;**15**: R29.

28. Subramanian A, Tamayo P, Mootha VK, Mukherjee S, Ebert BL, Gillette MA, Paulovich A, Pomeroy SL, Golub TR, Lander ES, Mesirov JP. Gene set enrichment analysis: A knowledge-based approach for interpreting genome-wide expression profiles. *Proceedings of the National Academy of Sciences* 2005;**102**: 15545-50.

29. Mootha VK, Lindgren CM, Eriksson K-F, Subramanian A, Sihag S, Lehar J, Puigserver P, Carlsson E, Ridderstrale M, Laurila E, Houstis N, Daly MJ, et al. PGC-1[alpha]-responsive genes involved in oxidative phosphorylation are coordinately downregulated in human diabetes. *Nat Genet* 2003;**34**: 267-73.

30. Matthews GM, Newbold A, Johnstone RW. Chapter Five - Intrinsic and Extrinsic Apoptotic Pathway Signaling as Determinants of Histone Deacetylase Inhibitor Antitumor Activity. In: Steven G. *Advances in Cancer Researche*d., vol. Volume 116: Academic Press, 2012: 165-97.

31. Xargay-Torrent S, Lopez-Guerra M, Saborit-Villarroya I, Rosich L, Campo E, Roue G, Colomer D. Vorinostat-induced apoptosis in mantle cell lymphoma is mediated by acetylation of proapoptotic BH3-only gene promoters. *Clinical cancer research : an official journal of the American Association for Cancer Research* 2011;**17**: 3956-68.

32. Boon K, Caron HN, van Asperen R, Valentijn L, Hermus MC, van Sluis P, Roobeek I, Weis I, Voute PA, Schwab M, Versteeg R. N-myc enhances the expression of a large set of genes functioning in ribosome biogenesis and protein synthesis. *The EMBO journal* 2001;**20**: 1383-93.

33. Hogarty MD, Norris MD, Davis K, Liu X, Evageliou NF, Hayes CS, Pawel B, Guo R, Zhao H, Sekyere E, Keating J, Thomas W, et al. ODC1 is a critical determinant of MYCN oncogenesis and a therapeutic target in neuroblastoma. *Cancer research* 2008;**68**: 9735-45.

34. Poortinga G, Wall M, Sanij E, Siwicki K, Ellul J, Brown D, Holloway TP, Hannan RD, McArthur GA. c-MYC coordinately regulates ribosomal gene chromatin remodeling and Pol I availability during granulocyte differentiation. *Nucleic acids research* 2011;**39**: 3267-81.

35. Brodeur GM, Pritchard J, Berthold F, Carlsen NL, Castel V, Castelberry RP, De Bernardi B, Evans AE, Favrot M, Hedborg F, et al. Revisions of the international criteria for neuroblastoma diagnosis, staging, and response to treatment. *Journal of clinical oncology : official journal of the American Society of Clinical Oncology* 1993;**11**: 1466-77.

36. Yanik GA, Parisi MT, Shulkin BL, Naranjo A, Kreissman SG, London WB, Villablanca JG, Maris JM, Park JR, Cohn SL, McGrady P, Matthay KK. Semiquantitative mIBG scoring as a prognostic indicator in patients with stage 4 neuroblastoma: a report from the Children's oncology group. *Journal of nuclear medicine : official publication, Society of Nuclear Medicine* 2013;**54**: 541-8.

37. Lonergan GJ, Schwab CM, Suarez ES, Carlson CL. Neuroblastoma, ganglioneuroblastoma, and ganglioneuroma: radiologic-pathologic correlation. *Radiographics : a review publication of the Radiological Society of North America, Inc* 2002;**22**: 911-34.

38. Reynolds CP, Matthay KK, Villablanca JG, Maurer BJ. Retinoid therapy of high-risk neuroblastoma. *Cancer letters* 2003;**197**: 185-92.

39. Fouladi M, Park JR, Stewart CF, Gilbertson RJ, Schaiquevich P, Sun J, Reid JM, Ames MM, Speights R, Ingle AM, Zwiebel J, Blaney SM, et al. Pediatric phase I trial and pharmacokinetic study of vorinostat: a Children's Oncology Group phase I consortium report. *Journal of clinical oncology : official journal of the American Society of Clinical Oncology* 2010;**28**: 3623-9.

40. Ferrari-Toninelli G, Bonini SA, Uberti D, Buizza L, Bettinsoli P, Poliani PL, Facchetti F, Memo M. Targeting Notch pathway induces growth inhibition and differentiation of neuroblastoma cells. *Neuro-oncology* 2010;**12**: 1231-43.

41. Rubie H, Hartmann O, Michon J, Frappaz D, Coze C, Chastagner P, Baranzelli MC, Plantaz D, Avet-Loiseau H, Benard J, Delattre O, Favrot M, et al. N-Myc gene amplification is a major prognostic factor in localized neuroblastoma: results of the French NBL 90 study. Neuroblastoma Study Group of the Societe Francaise d'Oncologie Pediatrique. *Journal of clinical oncology : official journal of the American Society of Clinical Oncology* 1997;**15**: 1171-82.

42. Shahbazi J, Liu PY, Atmadibrata B, Bradner JE, Marshall GM, Lock RB, Liu T. The bromodomain inhibitor JQ1 and the histone deacetylase inhibitor panobinostat synergistically reduce N-Myc expression and induce anticancer effects. *Clinical cancer research : an official journal of the American Association for Cancer Research* 2016.

43. Ecker J, Oehme I, Mazitschek R, Korshunov A, Kool M, Hielscher T, Kiss J, Selt F, Konrad C, Lodrini M, Deubzer HE, von Deimling A, et al. Targeting class I

histone deacetylase 2 in MYC amplified group 3 medulloblastoma. *Acta neuropathologica communications* 2015;**3**: 22.

44. Kong G, Hofman MS, Murray WK, Wilson S, Wood P, Downie P, Super L, Hogg A, Eu P, Hicks RJ. Initial Experience With Gallium-68 DOTA-Octreotate PET/CT and Peptide Receptor Radionuclide Therapy for Pediatric Patients With Refractory Metastatic Neuroblastoma. *Journal of pediatric hematology/oncology* 2015.

45. Goldberg JM, Glade-Bender J, Sulis ML, Gardner RA, Pollard JA, Aquino V, Winich NJ, Bostrom BC, Fu C, Hutchinson RJ, Manley TJ, Mody R, et al.: 3705 A Phase 1 Dose Finding Study of Panobinostat in Children with Hematologic Malignancies: Initial Report of TACL Study T2009-012 in Children with Acute Leukemia *American Society of Hematology Annual Meeting and Exposition* 2014.

46. San-Miguel JF, Hungria VT, Yoon SS, Beksac M, Dimopoulos MA, Elghandour A, Jedrzejczak WW, Gunther A, Nakorn TN, Siritanaratkul N, Corradini P, Chuncharunee S, et al. Panobinostat plus bortezomib and dexamethasone versus placebo plus bortezomib and dexamethasone in patients with relapsed or relapsed and refractory multiple myeloma: a multicentre, randomised, double-blind phase 3 trial. *The Lancet Oncology* 2014;**15**: 1195-206.

47. AACR. Panobinostat approved for multiple myeloma. *Cancer discovery* 2015;**5**: OF4.

48. Matthay KK, Villablanca JG, Seeger RC, Stram DO, Harris RE, Ramsay NK, Swift P, Shimada H, Black CT, Brodeur GM, Gerbing RB, Reynolds CP. Treatment of high-risk neuroblastoma with intensive chemotherapy, radiotherapy, autologous bone marrow transplantation, and 13-cis-retinoic acid. Children's Cancer Group. *The New England journal of medicine* 1999;**341**: 1165-73.

Figure Legends

Figure 1:

Panobinostat induces apoptosis in mouse neuroblastoma cells. **(A and B)** NH02A cells were treated with panobinostat, in the absence/presence of Q-VD-OPh, for 48 hr and the percentage of cells with sub-G1 DNA content determined. **(A)** Representative FACS plots of control, 50 nM panobinostat and 50 nM panobinostat with q-VD-OPh treated cells, while **(B)** shows quantitation of the results (mean ± SEM, n=3). **(C)** NH02A cells were treated for either 4 or 48 hr with vehicle or panobinostat. Protein lysates were immunoblotted for Acetyl-Histone H3, caspase 3 and actin as shown. **(D)** NH02A cells were treated with 50 nM panobinostat for 24hr, cytospun, fixed and stained for TUNEL assay reactivity, left panel shows quantitiation of results (mean ± SEM, n=3; **P*<0.05, *t*-test); right panel shows representative images. **(E)** NH02A cells were treated with 5 nM panobinostat for times shown. Protein samples were immunoblotted for BIM, Bcl-2, Mcl-1 and actin. **(F)**. RNA extracted from cells treated with 5 nM panobinostat for the times shown and analysed for BMF expression by RT-PCR. Results are expressed as mean BMF expression relative to baseline ± SEM, n=4 (** *P*<0.001 one-way ANOVA).

Figure 2:

Panobinostat prolongs survival and reduces tumour burden in TH-MYCN neuroblastoma mice. Tumour bearing homozygous TH-MYCN mice were randomized to receive vehicle or panobinostat for 3 or 9 weeks and monitored for disease recurrence. **(A)** Mean neuroblastoma tumour volume of each treatment group at randomisation (mean ± SEM, n=8-12 mice per group) as determined by ultrasound imaging measurements. A representative ultrasound image used for volumetric analysis of neuroblastoma *(inset*). **(B)** Individual tumour volumes of mice during the study (black, vehicle; red, 3 week treatment group; blue, 9 week treatment group). Dotted line represents a tumour volume of less than $50mm^3$, which on ultrasound imaging was assigned as 'below the limit of detection'. **(C)** Kaplan Meier survival analysis following treatment of tumour bearing mice with vehicle or 5 mg/kg panobinostat IP daily for either 3 or 9 weeks (black, vehicle; red, 3 week treatment group; blue, 9 week treatment group). Survival was defined as the time to an approved ethical endpoint for euthanasia. Dotted lines represent the last day of treatment for

that group. Mice were sacrificed when tumours relapsed and the experiment was ended at 100 days post end of treatment (*** $P<0.0001$ one-way ANOVA, 3 week and 9 week groups vs vehicle, and 3 week vs 9 week).

Figure 3:

Short term panobinostat treatment induces apoptosis in TH-MYCN neuroblastoma bearing mice. Tumour bearing mice (n=4/group) were treated with two doses of either vehicle or 5 mg/kg panobinostat 24 hr apart before being euthanized at 4 hr post dosing on day 2 (24 hr) and tumours collected for analysis. **(A)** Representative images of tumour sections stained for cleaved caspase 3 expression, TUNEL assay reactivity and H&E (40 x magnification). **(B)** Tumour lysates from all mice were immunoblotted for Acetyl-Histone H3, BMF, BIM, Mcl-1, Bcl-2 and actin. **(C)** RT-PCR analysis of tumour samples was undertaken for BMF mRNA expression. Results are shown as expression relative to that in vehicle treated tumours (mean ± SEM, n=4, *$P<0.05$, *t*-test).

Figure 4:

Panobinostat promotes differentiation in TH-MYCN driven tumours.

Tumours were analysed at baseline or days 7 and 21 of panobinostat treatment or at endpoint, 100 days after the cessation of treatment. Representative images are shown at each time point following staining with H&E, and for N-Myc, S100, SSTR2 and Enolase 2 (NSE) expression (40x magnification). Black arrows indicate ganglion cells, blue arrows indicate neuroblastoma cells.

Figure 5:

Differential expression and pathway analysis of TH-MYCN tumours in response to panobinostat. Tumour bearing mice (n=4/group) were harvested at baseline or 4 hr post panobinostat dosing on day 2 and tumours processed for RNA-seq and differential gene expression analysis. **(A)** GeneGo MetaCore pathway analysis showing the top ten significantly altered pathways in response to panobinostat treatment (Expression fold change threshold 0.25). **(B)** GSEA enrichment plot of the up-regulated genes (31 genes) from the Frumm differentiation gene signature, NES 1.56, FDR q-value 0.042. **(C)** Heat map of the expression of the 41 genes from the Frumm differentiation gene signature within the panobinostat TH-MYCN treated

tumours as compared to control samples (red up-regulated, blue down-regulated). Top panel, genes up-regulated within the Frumm gene signature; bottom panel, down-regulated genes. Genes are ranked by signal to noise ratio.

Figure 1

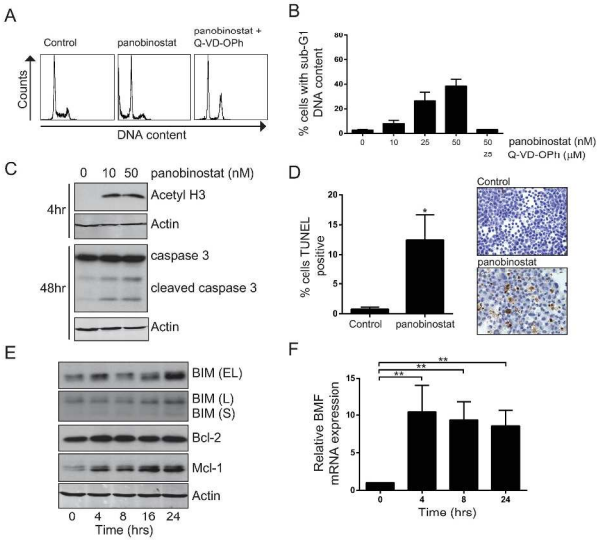

Figure 1
297x420mm (300 x 300 DPI)

Figure 2

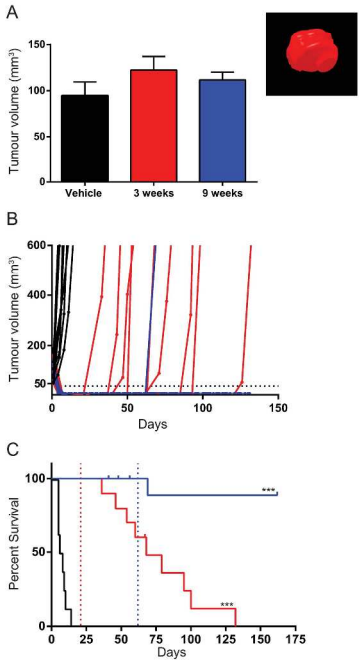

Figure 2
297x420mm (300 x 300 DPI)

Figure 3

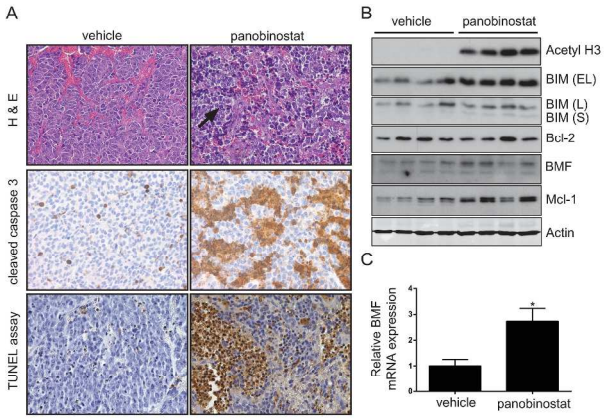

Figure 3
297x420mm (300 x 300 DPI)

Figure 4

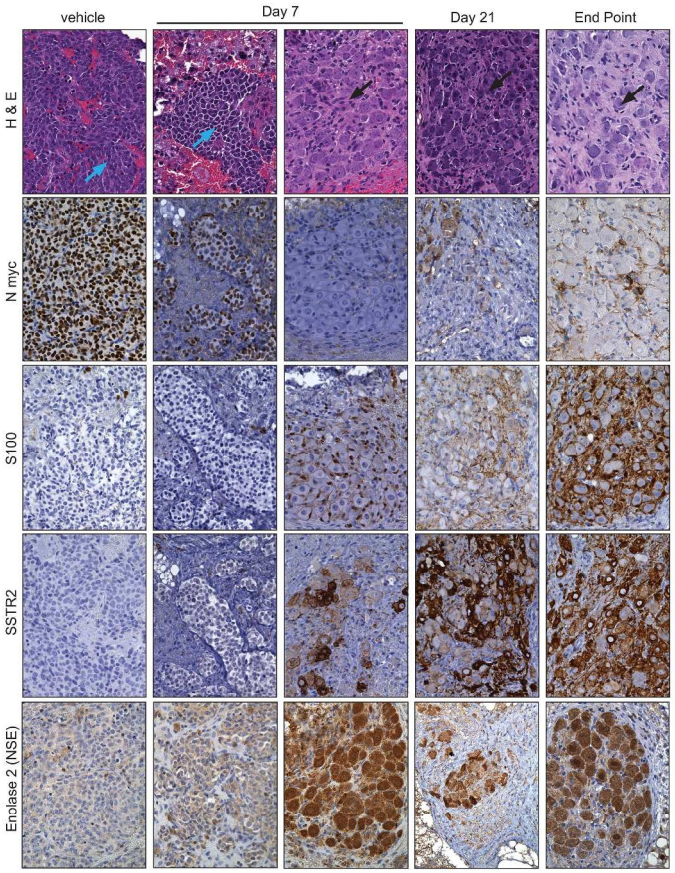

Figure 4
297x420mm (300 x 300 DPI)

Figure 5

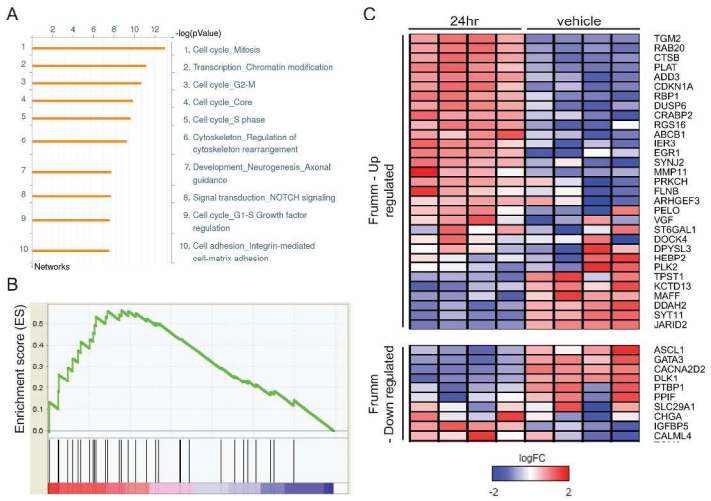

Figure 5
297x420mm (300 x 300 DPI)